The Role of Diffusion-Weighted Imaging and the Apparent Diffusion Coefficient (ADC) Values for Breast Tumors

Mi Jung Park, MD
Eun Suk Cha, MD
Bong Joo Kang, MD
Yon Kwon Ihn, MD
Jun Hyun Baik, MD

Objective: We wanted to evaluate the role of diffusion-weighted imaging (DWI) and the apparent diffusion coefficient (ADC) for detecting breast tumors, as compared with the T1- and T2-weighted images.

Materials and Methods: Forty-one female patients underwent breast MRI, and this included the T1-, T2-, DWI and dynamic contrast-enhanced images. Sixty-five enhancing lesions were detected on the dynamic contrast-enhanced images and we used this as a reference image for detecting tumor. Fifty-six breast lesions were detected on DWI and the histological diagnoses were as follows: 43 invasive ductal carcinomas, one mucinous carcinoma, one mixed infiltrative and mucinous carcinoma, seven ductal carcinomas in situ (DCIS), and four benign tumors. First, we compared the detectability of breast lesions on DWI with that of the T1- and T2-weighted images. We then compared the ADCs of the malignant and benign breast lesions to the ADCs of the normal fibroglandular tissue.

Results: Fifty-six lesions were detected via DWI (detectability of 86.2%). The detectabilities of breast lesions on the T1- and T2-weighted imaging were 61.5% (40/65) and 75.4% (49/65), respectively. The mean ADCs of the invasive ductal carcinoma ($0.89 \pm 0.18 \times 10^{-3}$ mm^2/second) and DCIS ($1.17 \pm 0.18 \times 10^{-3}$ mm^2/second) are significantly lower than those of the benign lesions ($1.41 \pm 0.56 \times 10^{-3}$ mm^2/second) and the normal fibroglandular tissue ($1.51 \pm 0.29 \times 10^{-3}$ mm^2/second).

Conclusion: DWI has a high sensitivity for detecting breast tumors, and especially for detecting malignant breast tumors. DWI was an effective imaging technique for detecting breast lesions, as compared to using the T1- and T2-weighted images.

Index terms:
Diffusion-weighted imaging
Breast, MR
Breast, cancer
Detectability

Korean J Radiol 2007;8:390-396
Received November 3, 2007; accepted after revision May 25, 2007.

Department of Radiology, St. Vincent's Hospital, The Catholic University of Korea, Suwon 442-723, Korea

Address reprint requests to:
Eun Suk Cha, MD, Department of Radiology, St. Vincent's Hospital, The Catholic University of Korea, 93-6 Ji-dong Paldal-gu, Suwon City 442-723, Korea.
Tel. (8231) 249-8495
Fax. (8231) 247-5713
e-mail: escha@catholic.ac.kr

Diffusion is the result of thermal fluctuations with a random pattern and this is often referred to as "Brownian motion" (1–3). Diffusion-weighted imaging (DWI) is the primary modality that's used to evaluate acute cerebral infarction. DWI has recently been widely used to evaluate other organs such as the ovaries, pancreas, prostate, liver and breast (2–10). Until now, there have been few reports published about using the DWI technique to detect and characterize breast tumors, and especially malignant breast tumor (2–5).

Breast MRI has widely used for the detection, diagnosis and staging of breast cancer (11–14). T1- and T2-weighted images are routinely performed before dynamic contrast-enhanced imaging. Although the T1- and T2-weighted images can show a tumor's structure and the tissue component, these modalities have some limitations for detecting and characterizing breast lesions. As DWI identifies the biologic characteristics of tissue, we expected that DWI would provide more useful information for

detecting breast tumors (1). We also hypothesized that DWI has a topographic role, and it may replace the T1- and T2-weighted imaging, for the detection of breast tumors. We have also discussed the possibility of DWI replacing dynamic-enhanced imaging if the latter is contraindicated because of a patient's allergy and/or the expense of contrast media (5). The apparent diffusion coefficient (ADC) values are measured to estimate the degree of diffusion (1). Some authors have reported lower ADC values for breast cancer compared with normal fibroglandular tissue (2–5). Therefore, we have previously discussed the usefulness of ADC values for detecting breast cancer (2–5).

To demonstrate the role of the DWI, we analyzed the ability of each pulse sequences to detect breast lesions (the T1-, T2-, DWI and dynamic contrast-enhanced MR images), and we then analyzed the ADCs values of both malignant and benign breast lesions and the normal fibroglandular tissue.

MATERIALS AND METHODS

Subjects

This study includes 41 women (mean age: 53.1 years, age range: 30–70 years) who underwent breast MRI from June 9, 2005 to September 21, 2005 because of suspicious mammographic or ultrasonographic abnormalities. Sixty-five pathologically-proven breast lesions were detected on the dynamic contrast-enhanced imaging. Fifty-six lesions were confirmed from the surgically excised specimens and these specimens were excised via modified radical mastectomy or lumpectomy, and nine lesions were confirmed from core needle biopsy.

Histopathologic Data

Nine of 65 lesions were not detected on DWI and all of the nine lesions were confirmed to be invasive ductal carcinoma. Fifty-six of the 65 lesions were detected on DWI. There were 52 malignant lesions, including 43 invasive ductal carcinomas, one mucinous carcinoma, one mixed infiltrative and mucinous carcinoma, and seven DCIS. There were four benign lesions, including one fibroadenoma, one epidermal inclusion cyst and two cases of fibrocystic disease. The mean diameter of the breast lesions was 2.46 cm with a range from 0.6 cm to 13.1 cm.

MRI Protocol

The images were acquired with a 1.5-T scanner (GE Signa Excite Twin Speed, GE Medical Systems, Milwaukee, WI). To minimize the respiratory motion artifacts, the patients were placed in the prone position and MRI was performed using the following sequences: sagittal fat-suppressed fast spin-echo T2-weighted imaging (TR/TE= 4000/85, a flip angle of 90°, 30 slices with a field of view [FOV] of 240 mm, a matrix of 256×224, 2 number of excitation [NEX] and a 3 mm section thickness with a 0.1 mm intersection gap, an acquisition time of 2 minutes 56 seconds); the axial DWI with single-shot echo-planar imaging (EPI) (b value = 0 and 1000 second/mm^2, TR/TE= 6000/75, a FOV of 360 mm, a matrix of 128 × 128, 2 NEX, a 4 mm section thickness with a 1 mm intersection gap, an acquisition time of 1 minute 30 seconds); and the pre- and post-contrast axial spin-echo T1-weighted imaging with TR/TE = 625/12, a flip angle of 90°, 31 slices with a FOV of 300 mm, a matrix of 256 × 192, 1.5 NEX and an acquisition time of 3 minutes 60 seconds. After DWI in the axial plane, a postcontrast sagittal T1-weighted three-dimensional, fat-suppressed, fast gradient spoiled sequence (TR/TE = 6.2/3.1, a flip angle of 10°, 2.6 mm section thickness, an acquisition time of 1 minute 31 seconds) was obtained before and 0, 91, 182, 273, 364 and 455 seconds after a rapid bolus injection of 0.1 mmol/kg body weight of Gd-DTPA (Magnevist, Schering, Berlin, Germany). The subtraction images were obtained by subtracting the precontrast images from the six series of post-contrast images on a pixel-by-pixel basis. We evaluated the breast lesions with using the T1- and T2-weighted imaging and the post-contrast T1-weighted, fat-suppressed, fast gradient spoiled sequence with maximal intensity projection (MIP). The computed mean ADCs of the breast lesions were then correlated.

Comparing the Detectability of Breast Tumors on Diffusion Weighted Imaging with that of the T1- and T2-weighted Imaging

Three radiologists separately counted the number of the breast lesions on the T1- and T2-weighted imaging, the DWI and the dynamic-enhanced imaging. We used dynamic-enhanced imaging as a reference for detecting tumor at the time of evaluation. On the T1- and T2-weighted image, the regions were selected as being identifiable compared to the normal fibroglandular tissue. The relative percentage of detected tumor was calculated for the T1- and T2-weighted imaging and the DWI. Finally, we compared the detectability of breast tumors on each pulse sequence.

Diffusion Image Acquisition and Apparent Diffusion Coefficients Analysis

Diffusion weighted imaging was obtained in each of the x, y and z axes. The ADC was calculated according to ADC = (1/b2-b1) ln (S2/S1), where S1 and S2 are the

signal intensities in the regions of interest (ROI) obtained with different gradient factors (b values of 0 and 1000 s/mm^2). The ADC distribution was demonstrated on an axial ADC color map. The regions selected as being clearly identifiable had high-signal intensity on the DWI, yet we avoided the region of high signal intensity on the T2 weighted image to exclude the T2 shine-through effect. The ROIs were always placed within the actual mass, and the diameter of the ROI was 10 $\pm$ 2 mm^2. As a reference, we used the fibroglandular tissue that appeared as homogeneous signal intensity on both the ADC map and the T1-weighted images. The ADC values were automatically measured by drawing the ROIs. One radiologist calculated the ADC values twice, along with the change of location, and then she averaged these values.

To determine the ADC values of the breast tumor and normal fibroglandular tissue, we obtained images of 56 breast lesions on DWI and we measured the ADC values of each breast lesion. According to the histopathologic results, we categorized the breast tumors into three groups, i.e., invasive ductal carcinoma, DCIS and benign lesions, and the ADC values were then averaged. We excluded the non-invasive ductal carcinomas such as mucinous carcinoma and the mixed infiltrative and mucinous carcinoma because the samples' sizes were too small. We also compared the ADC values among the three groups and the normal fibroglandular tissue.

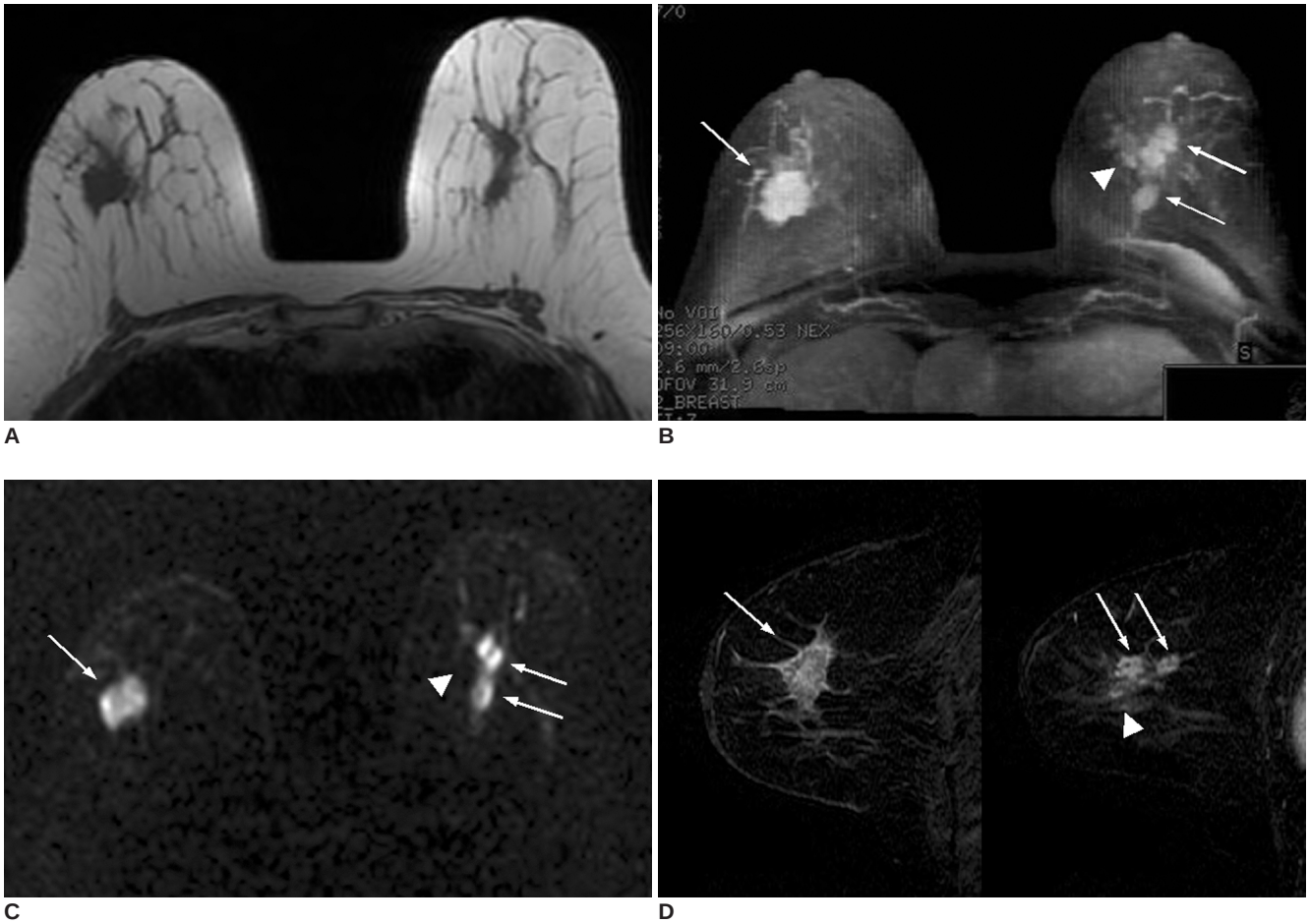

Fig. 1. A 69-year-old woman with bilateral invasive ductal carcinoma.
A. The axial T1-weighted image shows multiple lobular homogeneous iso-signal intensity masses in both breasts.
B. The maximum-intensity projection of the subtraction image shows multiple enhancing masses in both breasts (thin white arrows and arrowhead).
C. The axial diffusion weighted image shows multiple high-signal intensity masses in both breasts (thin white arrows), but tiny multicentric lesions are not detected in the left breast (white arrowhead). The apparent difusion coefficient value of the right breast tumor was 0.94 $\times 10^{-3}$ mm^2/second and that of the left breast tumor was 0.84 $\times 10^{-3}$ mm^2/second.
D. The sagittal dynamic-enhanced T1-weighted gradient-echo substraction image of the first postcontrast acquisition shows multiple, heterogeneous, rim-enhancing masses in both breasts (thin white arrows and white arrowhead). The left side of this image represents the right breast and the right one represents the left breast. A tiny multicentric lesion is extremely well visualized in the left breast (white arrowhead).

Statistics

T-tests were used for analyzing the differences of the mean ADC values of the invasive ductal carcinoma, DCIS and normal fibroglandular tissue. For comparison of the small groups, the Mann-Whitney test was used to compare the mean ADC values between the benign breast lesions and the normal breast parenchyma.

RESULTS

Comparing the Detectability of Breast Tumors on Diffusion Weighted Images with the that of the T1- and T2-weighted Images

Sixty-five enhancing lesions were detected on the dynamic contrast-enhanced images. Fifty-six lesions were detected on DWI (a detectability rate of 86%). The T1- and T2-weighted imaging detected 62% (40/65) and 75% (49/65) of the lesions, respectively (Table 1).

Nine of 65 enhancing lesions were not detected on DWI (14%). Eight of these nine lesions were confirmed to be daughter nodules of the malignant lesions (Fig. 1), and one of the nine lesions was not visualized due to technical problems.

Table 1. The Tumors Detected on Each Pulse Sequence out of 65 Tumors that were seen on the Contrast Enhanced Images

	Detection Number (Rate %)
T1	40 / 65 (61.5%)
T2	49 / 65 (75.4%)
Diffusion weight image	56 / 65 (86.2%)

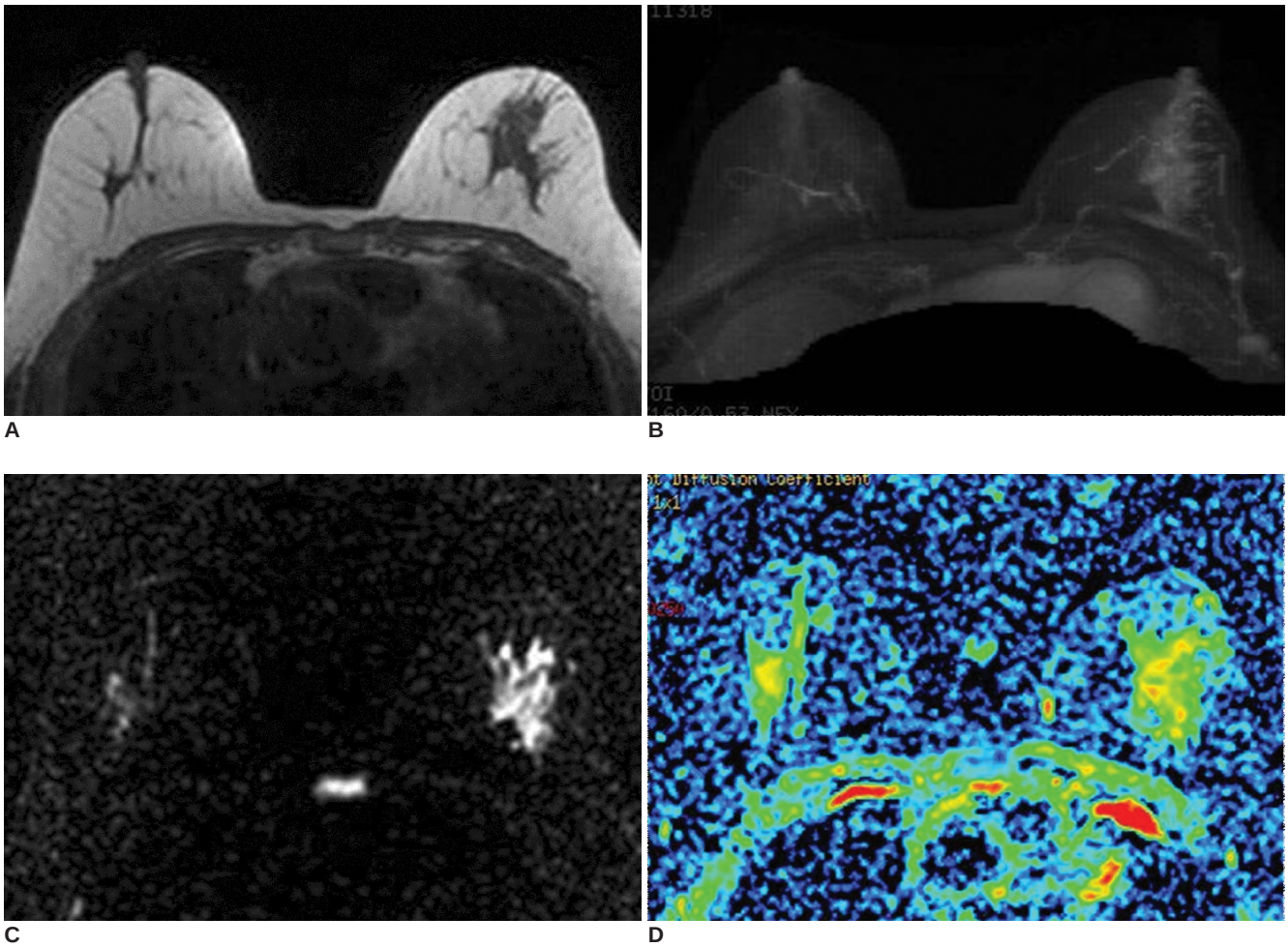

Fig. 2. A 53-year-old woman with ductal carcinoma in situ.
A. The axial T1-weighted image shows segmentally distributed, asymmetric, iso-signal intensity, non-mass lesion in the left breast.
B. The maximal intensity projection of a subtraction image shows heterogeneous clumpy enhancement in the left breast.
C. The diffusion-weighted image shows the main lesion to be a high-signal intensity lesion.
D. The axial plane apparent diffusion coefficient map shows a mixed green and yellow area and the apparent diffusion coefficient value of this breast tumor was 1.43×10^{-3} mm²/second.

Comparing the ADC Values of the Invasive Ductal Carcinoma, DCIS, the Benign Lesions and the Normal Fibroglandular Tissue

The mean ADC value of each type of lesion was invasive ductal carcinoma: 0.89 $\pm$ 0.18 $\times 10^{-3}$mm^2/second, DCIS: 1.17 $\pm$ 0.18 $\times 10^{-3}$mm^2/second, benign lesions: 1.41 $\pm$ 0.56 $\times 10^{-3}$mm^2/second and normal breast parenchyma: 1.51 $\pm$ 0.29 $\times 10^{-3}$mm^2/second (Table 2, Figs. 1–3). We excluded the ADC value of noninvasive ductal carcinomas such as one mucinous carcinoma and the one mixed infiltrative and mucinous carcinoma. The mean ADCs of the invasive ductal carcinoma and DCIS were significantly lower than that of the normal fibroglandular tissue ($p < 0.05$). Also, the mean ADC of the DCIS was statistically higher than that of the invasive ductal carcinoma ($p < 0.05$). In addition, the difference of the mean ADC values between invasive ductal carcinoma and the benign breast lesions was significant ($p < 0.05$) according to the Mann-Whitney test.

Table 2. The Distribution of the ADC Values for IDC, DCIS, Benign Lesions and Normal Fibroglandular Tissue

	N	ADC Values (10^{-3} mm^2/second)
IDC	43	0.89 $\pm$ 0.18
DCIS	7	1.17 $\pm$ 0.18
Benign lesions	4	1.41 $\pm$ 0.56
Fibroglandular tissue	41	1.51 $\pm$ 0.29

Note.—ADC = apparent diffusion coefficient, IDC = invasive ductal carcinoma, DCIS = ductal carcinoma in situ

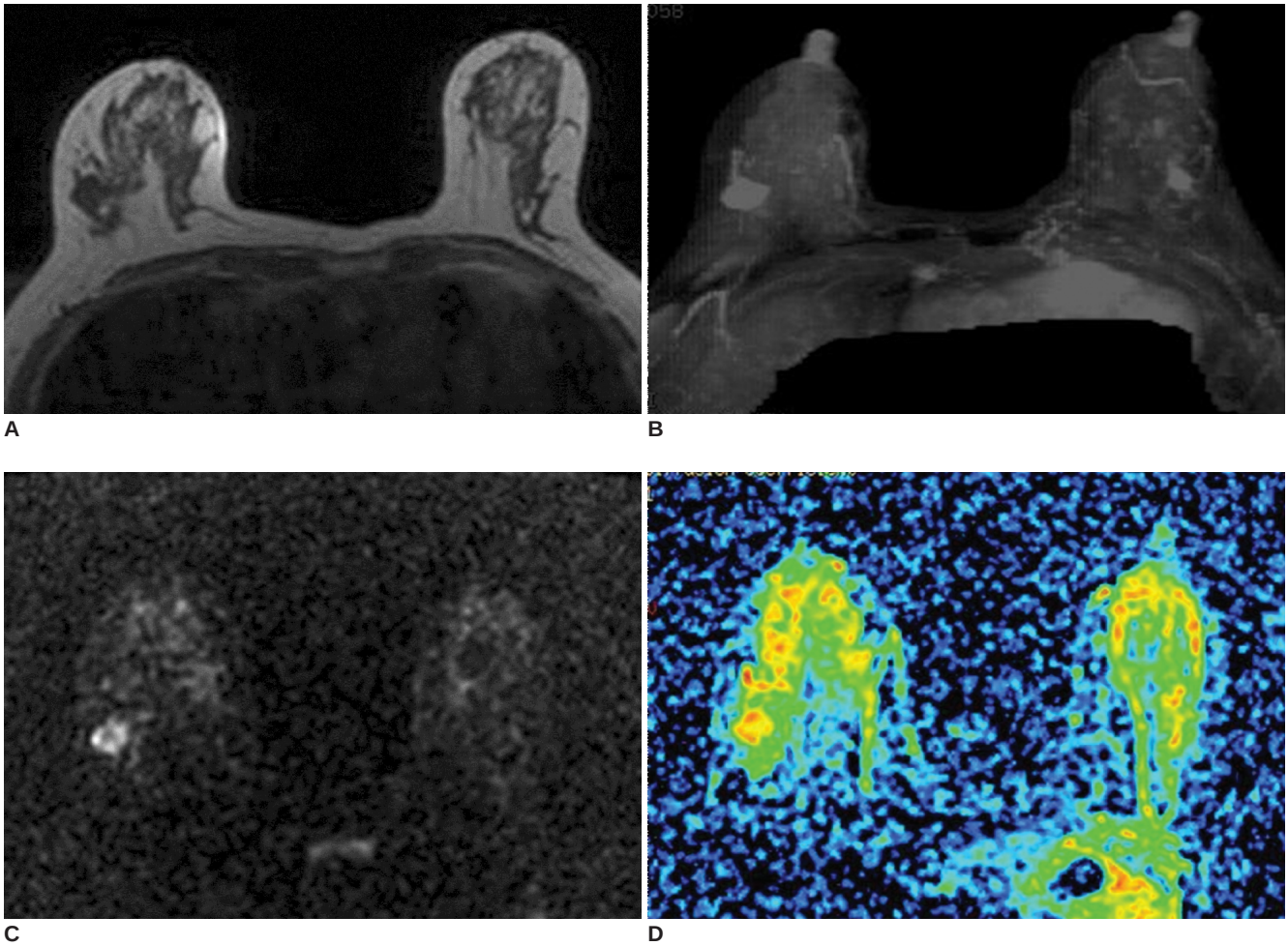

Fig. 3. A 41-year-old woman with fibroadenoma that was confirmed by core-needle biopsy.
A. The axial T1-weighted image shows a circumscribed oval iso-signal intensity mass in the right breast.
B. The maximal intensity projection of the subtraction image shows homogeneous enhancement in the right breast. A nonspecific small enhancing nodule is also seen in the left breast. This left nodule showed typical benign features on the breast USG (not shown), so we did not perform core-needle biopsy.
C. The diffusion-weighted image shows the mass to be a high-signal intensity lesion in the right breast.
D. The axial plane apparent diffusion coefficient map shows the mixed yellow and red area, and the apparent diffusion coefficient value of this tumor was 1.63 $\times 10^{-3}$ mm^2/second.

DISCUSSION

Breast MRI is the widely accepted diagnostic approach for evaluating the breast (11). To improve the sensitivity of detecting breast cancer, several diverse techniques are used for breast MRI (11). In particular, dynamic-enhanced MRI provides for evaluating multiple foci of carcinoma in the breast and it displays extremely high sensitivity for identifying breast cancer (11, 12, 14–16). However, dynamic-enhanced breast MRI has some disadvantages such as being time-consuming and costly, the possible side effects of the contrast media and the relative low specificity compared to mammography and ultrasonography (11, 12, 14–16).

Generally in biologic tissues, microscopic motion includes both the molecular diffusion of water and the blood microcirculation in the capillary network, and both diffusion and perfusion affect the ADC values (1, 4, 5). Because of the extent of microvessels in malignant breast tumor, the ADC value can be strongly affected by perfusion when the b value is small (1, 4, 5). A previous report insisted that b-values less than 750 s/mm^2 are most effective for detecting breast tumors (5). However, we used single-shot EPI with a higher b-value (1,000 s/mm^2) so we could obtain diffusion effects without any significant image distortion (1, 3, 5).

The conventional T1- and T2-weighted images are routinely obtained for performing breast MRI before the contrast-enhanced MRIs are taken. Until now, the usefulness of the conventional T1- and T2-weighted images has been limited because small lesion is not detected in dense breast parenchyma and there is relatively low contrast resolution between the fibroglandular tissue and the breast lesion (13). In our study, DWI showed higher detectability for breast tumors than the T1- and T2-weighted images, although it showed lower detectability for breast tumors than the dynamic contrast-enhanced images.

In our study, out of the nine lesions that were not detected on DWI, eight were found to be daughter nodules of breast cancer. The mean size of these daughter nodules was 0.55 cm in diameter (range: 0.4 to 0.8 cm). A previous report demonstrated that nodules less than 1.0 cm in diameter are not detectable on DWI (4). One remaining nodule of the nine lesions was not detected due to chemical shift artifact, despite its relatively large size (1.4 cm), because the chemical shift artifact caused incorrect information about the lesion's location. Therefore, DWI will not perfectly replace contrast-enhanced imaging; however, DWI is a better method for detecting breast tumors compared to T1- and T2-weighted imaging if contrast-enhanced imaging is contraindicated (17, 18).

Several studies have measured the ADCs of breast lesions with using DWI (2–5). The data from these studies has shown discrepancies in the ADC values along the b values. For example, the mean ADCs of the malignant lesions were $1.60 \pm 0.36 \times 10^{-3}$ mm^2/second using b = 400 by Sinha et al. (3), $1.22 \pm 0.19 \times 10^{-3}$ mm^2/second using b = 700 by Kinoshita et al. (4), $1.12 \pm 0.24 \times 10^{-3}$ mm^2/second using b = 750 by Woodhams et al. (5), and $0.97 \pm 0.20 \times 10^{-3}$ mm^2/second using b = 1,000 by Guo et al. (2). The reason for these discrepancies can be explained by the fact that the ADCs were determined with using linear regression analysis and analysis of the natural log of the signal intensity versus the gradient factor (b) (1, 6). Our results show that the mean ADC of a malignant lesion is $0.89 \pm 0.18 \times 10^{-3}$ mm^2/second, which is well correlated with the above-mentioned results. We recommend that the ADC value of breast lesions be compared to that of normal fibroglandular tissue because the ADC value was variable according to the gradient factor. Our results show that the mean ADCs of invasive ductal carcinoma and DCIS are significantly lower than that of normal fibroglandular tissue ($p < 0.05$).

Our study has some limitations. First, the number on the benign lesions was very small to make comparison with malignant lesions. We usually perform DWI for the purpose of preoperatively evaluating suspected breast cancer. Therefore, we could not obtain a sufficient number of benign breast lesions. Previous reports have stated that the diffusion imaging is useful to differentiate malignant breast lesion from benign lesion (2, 4). Secondly, we could only perform non-parameter testing on the normal fibroglandular tissue distribution. Despite that we attempted to obtain the ADC values in the normal fibroglandular tissue, some regions were mixed up with the breast tumors, and this was especially true for the intraductal spread of breast lesions. Thirdly, we could not detect daughter nodules, and especially those that were less than 1.0 cm in diameter. In our study, we used a slice thickness of 1 cm for DWI, but we used a slice thickness of 3 mm for the dynamic contrast-enhanced imaging (4).

In conclusion, DWI is a better method for detecting breast tumors than either T1- or T2-weighted imaging, but DWI should be performed in conjunction with contrast-enhanced MRI because it is evident that small breast lesions are not seen on DWI. In addition, the DWI is an effective screening technique. We can obtain DWI with a one-minute scan time. The ADC value is useful to differentiate malignant breast lesion from normal breast fibroglandular tissue. Yet the ADC value is variable according to the gradient factor, and it should be compared with that of

the normal fibroglandular tissue.

References

1. Bammer R, Basic principles of diffusion-weighted imaging. *Eur J Radiol* 2003;45:169-184
2. Guo Y, Cai YQ, Cai ZL, Gao YG, An NY, Ma L, et al. Differentiation of clinically benign and malignant breast lesions using diffusion-weighted imaging. *J Magn Reson Imaging* 2002;16:172-178
3. Sinha S, Lucas-Quesada FA, Sinha U, DeBruhl N, Bassett LW. In vivo diffusion-weighted MRI of the breast: potential for lesion characterization. *J Magn Reson Imaging* 2002;15:693-704
4. Kinoshita T, Yashiro N, Ihara N, Funatu H, Fakuma E, Narita M. Diffusion-weighted half-Fourier single-shot turbo spin echo imaging in breast tumor: differentiation of invasive ductal carcinoma from fibroadenoma. *J Comput Assist Tomogr* 2002;26:1042-1046
5. Woodhams R, Matsunaga K, Iwabuchi K, Kan S, Hata H, Kuranami M, et al. Diffusion-weighted imaging of malignant breast tumors: the usefulness of apparent diffusion coefficient (ADC) value and ADC map for the detection of malignant breast tumors and evaluation of cancer extension. *J Comput Assist Tomogr* 2005;29:644-649
6. Kim T, Murakami T, Takahashi S, Tsuda K, Nakamura H. Diffusion-weighted single-shot echoplanar MR Imaging for liver disease. *AJR Am J Roentgenol* 1999;173:393-398
7. Ichikawa T, Haradome H, Hachiya J, Nitatori T, Araki T. Diffusion-weighted MR imaging with a single-shot echoplanar sequence: detection and characterization of focal hepatic lesions. *AJR Am J Roentgenol* 1998;170:397-402
8. Yamashita Y, Namimoto T, Mitsuzaki K, Urata J, Tsuchigame T, Takahashi M, et al. Mucin-producing tumor of the pancreas: diagnostic value of diffusion-weighted echo-planar MRI imaging. *Radiology* 1998;208:605-609
9. Moteki T, Ishizaka H. Diffusion-weighted EPI of cystic ovarian lesions: evaluation of cystic contents using apparent diffusion coefficients. *J Magn Reson Imaging* 2000;12:1014-1019
10. Hosseinzadeh K, Schwarz SD. Endorectal diffusion-weighted imaging in prostate cancer to differentiate malignant and benign peripheral zone tissue. *J Magn Reson Imaging* 2004;20:654-661
11. Bluemke DA, Gatsonis CA, Chen MH, DeAngelis GA, DeBruhl N, Harms S, et al. Magnetic resonance imaging of the breast prior to biopsy. *JAMA* 2004;292:2735-2742
12. Orel SG, Schnall MD. MR imaging of the breast for the detection, diagnosis, and staging of breast cancer. *Radiology* 2001;220:13-30
13. DeBruhl ND, Michael D, Bassett LW. *Magnetic resonance imaging of breast tumors*. In: Bassett LW, Jackson VP, Fu KL, Fu YS, eds. *Diagnosis of diseases of the breast*, 2nd ed. Philadelphia: Elsevier Saunders, 2005:225-250
14. Ikeda DM, Baker DR, Daniel BL. Magnetic resonance imaging of breast cancer : clinical indications and breast MRI reporting system. *J Magn Reson Imaging* 2000;12:975-983
15. Siegmann KC, Müller-Schimpfle M, Schick F, Remy CT, Fersis N, Ruck P, et al. MR imaging-detected breast lesion: histopathologic correlation of lesion characteristics and signal intensity data. *AJR Am J Roentgenol* 2002;178:1403-1409
16. Jacobs MA, Barker PB, Bluemke DA, Maranto C, Arnold C, Herskovits EH, et al. Benign and malignant breast lesions: diagnosis with multiparametric MR imaging. *Radiology* 2003;229:225-232
17. Warach S, Boska M, Welch KM. Pitfalls and potential of clinical diffusion-weighted MR imaging in acute stroke. *Stroke* 1997;28:481-482
18. Sugahara T, Korogi Y, Kochi M, Ikushima I, Shigematu Y, Hirai T, et al. Usefulness of diffusion-weighted MRI with echo-planar technique in the evaluation of cellularity in gliomas. *J Magn Reson Imaging* 1999;9:53-60